JOURNAL PRE-PROOF

This is an early version of the article, published prior to copyediting, typesetting, and editorial correction. The manuscript has been accepted for publication and is now available online to ensure early dissemination, author visibility, and citation tracking prior to the formal issue publication.

It has not undergone final language verification, formatting, or technical editing by the journal's editorial team. Content is subject to change in the final Version of Record.

To differentiate this version, it is marked as "PRE-PROOF PUBLICATION" and should be cited with the provided DOI. A visible watermark on each page indicates its preliminary status.

The final version will appear in a regular issue of *Engineering Transactions*, with final metadata, layout, and pagination.

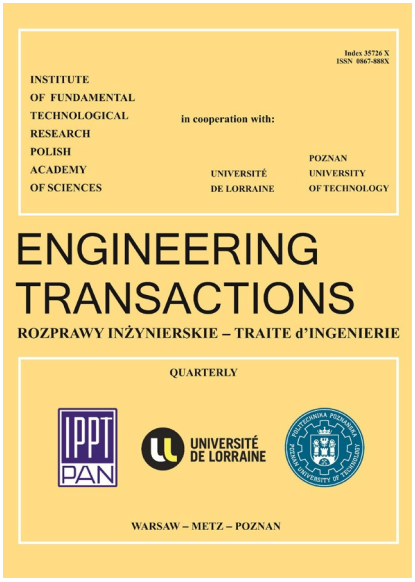

Title: Analytical Approach and Shooting Method Solution of Nonlocal Eringen Elasticity Problem of Nanorods

Author(s): Aleksandra Manecka-Padaż, Ewa Eliza Rożko, Zdzisław Nowak, Piotr Chudzinski

DOI: https://doi.org/10.24423/engtrans.2025.3681

Journal: *Engineering Transactions*

ISSN: 0867-888X, e-ISSN: 2450-8071

Publication status: In press

Received: 2025-10-31

Revised: 2025-12-01

Accepted: 2025-12-06

Published pre-proof: 2025-12-12

Please cite this article as:

Manecka-Padaż A., Rożko E.E., Nowak Z., Chudzinski P., Analytical Approach and Shooting Method Solution of Nonlocal Eringen Elasticity Problem of Nanorods, *Engineering Transactions*, 2025, https://doi.org/10.24423/engtrans.2025.3681

Analytical Approach and Shooting Method Solution of Nonlocal Eringen Elasticity Problem of Nanorods

Aleksandra MANECKA-PADAŻ[1*], Ewa Eliza ROŻKO[1,2],
Zdzisław NOWAK[1], Piotr CHUDZINSKI[1]

[1]Institute of Fundamental Technological Research, Polish Academy of Sciences, Warsaw, Poland
[2] Institute of Outcomes Research, Maria Sklodowska-Curie Medical Academy, Warsaw, Poland

*Corresponding Author e-mail: amanecka@ippt.pan.pl

The aim of this paper is to study the postbuckling behaviors of the nanorods combined with the small scale effects. In this paper, buckling of a nanorod column subjected to tip load is investigated. The nanorod is on a clamped support at one end, while the other end is simply-supported subjected to axial compression. At this end, the nanorod is movable only in a horizontal direction. The governing differential equation describing the behavior of the nanorod is developed by the moment–curvature relationship in analogy with the classical Euler–Bernoulli beam theory together with the equilibrium equations, including the effects of nonlocal elasticity as well as corresponding boundary conditions. The numerical shooting methods are derived and employed to solve the differential equations in this problem. The results, including nonlocal elasticity, reveal that nanorods have decreased structural stiffness and show the significant effect of geometrical parameters on the stability of buckled nanorods, emphasizing the importance of accounting for their interaction in the design of nanostructural systems.

Keywords: nonlocal elasticity theory; nanorods; small-scale effect; postbuckling behaviors.

1. Introduction

For a slender elastic beam under axial compression, the classical Euler theory predicts a bifurcation of the straight configuration of the beam when the critical load is reached. The elastica problem was experimentally investigated by Pieter van Musschenbrock [1] and then mathematically studied by Daniel Bernoulli and Leonard Euler [2]. Finally it was solved by Euler [3] in 1744 who obtained 9 classes of solutions of the elastic curve and named it elasticaes. Motivated by recent progress in experiments on nanorods, here we study how these elasticaes are changing upon adding to the model nonlocality described by a single nonlocal parameter μ.

Over the years many researchers were interested in the elastica problem and there exist many studies focused on various aspects of this issue. Kirchhoff [4] found the analogy between the equations describing the equilibrium state of an elastic rod and those describing the dynamics of a simple swinging pendulum. Max Born [5] has studied the exact elasticaes curves in his PhD thesis. Nishinari [6] partially analyzed the nonlinear dynamics of elastic rods and applied the soliton approach to analyse the nonlinear deformation of real elastic rods, and to clarify the meaning of their assumption of velocities from the physical point of view. Chucheepsakul and Monprapussorn [7] studied a highly nonlinear problem of instability of a flexible elastic pipe transporting fluid. They based on the inextensible elastica theory of rod and solution is obtained by using the elliptic integrals and the numerical shooting method. Vassilev *et al.* [8] presented

the fluid membrane equilibrium shape equation in the form of a generalization of Euler's elastica. Kibach *et al.* [9] investigated the post-buckled free vibration problem of an elastica around one of its vibration modes. The main contribution of this article is the detection of nonlinear frequencies of the elastica, i.e. its different backbone curves, around one of its post-buckled configurations without any assumption on the order of magnitude of the curvature, the rotation and also of the response. The detected nonlinear frequency relationship provide tools for tuning parameters of the elastica in order to present special types of behaviours around one of its buckling and vibration modes. In paper by Taloni *et al.* [10] a general expression for the strain energy of a homogeneous, isotropic, plane extensible elastic with an arbitrary undeformed configuration is derived. This expression appears to be suitable for one-dimensional models of polymers or vesicles, the natural configuration of which is characterized by locally changing curvature. They discuss the relevance of their model in describing real biological non-homogeneous filaments. Leanza *et al.* [11] determined the axial buckling behavior for an elastic beam or rod which has a uniform curvature in its natural state, which in the elastica problem significantly enriches the variety of buckling behaviors exhibited by the rod or beam with straightened by pure bending, and clamped at its ends. While the classical elastica displays stable post-buckling behavior, the elastica with natural curvature exhibits a wide range of behaviors from stable to highly unstable. The stability of the interesting limit in which the maximum uniform natural curvature is imposed on a rod or beam clamped at both ends has also been determined via the initial post-bifurcation analysis. Phungpaingam and Chucheepsakul [12] analyzed the behavior of a variable-arc-length elastica subjected to the end loading with a rotational spring joint within the span length of the elastica. Lai *et al.* [13] investigated the buckling behavior of the compression of the high strength concrete encased steel columns including experimental, numerical and analytical analyses. Wang *et al.* [14] studied instability of an elastica under bilateral displacement control at a material point. Fraldia *et al.*[15] studied both compressive and tensile buckling in case of the human fingers luxation. It is shown that bifurcation in natural systems can be explained. Hathaipichitchai *et al.* [16] investigated the post-buckling behaviors of a variable-arc-length elastica pipe caused by internal transporting fluid motion including effect of pressure variability. Curatolo*et al.*[17] employed a modified Euler elastica model for optimizing catapult mechanism conditions due to the catapult emerging in a soft rod. Wang and Qiu [18] proposed an extended elastica-plastica theory for the Euler-Bernoulli beams. Shigeki Matsutani [19] studies the mechanics of elastica as a model of the shapes of the supercoiled DNA. The elastica problem was intensively investigated over the years and played a major role in the development of mathematics, including Jacobi elliptic functions and also numerical methods.

In recent decades, nanotechnology has been the main subject of interest for researchers from all over the world. Materials such as thin films, nanorods and nanotubes may exhibit unusual properties not noticed at the macroscale Duan *et al.* [20]. Modeling and optimization of the devices in nanoscale requires an extension characterization of the material in such a small scale. The elastica issue in nanoscale has also become of great interest in a long time. Wang and Feng [21] measured the mechanical properties of compressed nanowires based on the Euler buckling model. Moradi *et al.*[22] examined the mechanical behavior of polystyrene nanorods using the classical Euler-Bernoulli beam model.

Recently, further studies in nanoscale were undertaken, mainly based on the Eringen nonlocal theory of the elasticity. Nonlocal theory by Eringen assumes that the stress at a point is a function of the strains of adjacent points in the continuum Liu Mei [23]. This approach became an efficient tool for the analysis of the influence of the size effects in small scale structures. Thongyothee and Chucheepsakul [24] investigated the stability analysis of nanobeams including small-scale effects and surface stress. Challamel *et al.* [25] studied the elastica problem using an equivalent nonlocal continuum approach and comparing it with a discrete physical model. Lembo [26] have researched post-buckling configurations of nanorods with various end conditions using Eringen's nonlocal theory. Comparison of results for nonlocal and classical rods shows significant impact of the nonlocal parameter for the post-buckling behavior of the rod. Tang and Qing [27] numerically examined effects of the nonlocal parameters on static bending, elastic buckling and free vibration of Timoshenko beams under different boundary and loading conditions. Their study shows that a consistent softening effect can be obtained. Hussain and Naeem [28] applied Erinngen's theory to calculate the frequency of single wall carbon nanotubes (SWCNT). The outcome reveals that increasing the nonlocal parameter results in significantly reducing the natural frequencies of the SWCNT. Berecki *et al.* [29] compares Eringen's two-phase local/nonlocal model and Eringen's differential model in order to perform bifurcation analysis of a nanotube through which it passes a nanostring.It is also worth mentioning that an interesting result was obtained using the integral form of the nonlocal elasticity theory, such as stress-driven. Darban *et al.* [30], investigated size-dependent buckling of cracked nanocantilevers and the results can be applicable in a wide range of mechanical nanosensors. In [31], Darban analyzed nonuniform beams with multiple sub-beams. The model is based on stress-driven nonlocal theory and can be applied to control the flexural response of a nanobeam. In [32], Darban's approach provides explicit solutions for displacements and deflections, showing how size effects alter beam stiffness and behavior relative to classical theory using a variational approach and a transfer matrix method.

Although Eringen's nonlocal theory provides valuable analytical frameworks, most practical problems—especially those involving complex boundary conditions or nonlinear constitutive terms—require robust numerical techniques for their solution. Several computational methods have therefore been developed and applied to the nonlocal elasticity framework. Finite Difference and Finite Element Methods (FDM and FEM) remain the most frequently used numerical tools for static and dynamic analyses of nonlocal beams and plates, as reported by Reddy *et al.* [33] and Phadikar and Pradhan [34]. The Differential Quadrature Method (DQM) has also been implemented successfully for solving higher-order nonlocal governing equations, providing excellent accuracy for small-scale effects Aydogdu [35]. In addition, variational and Galerkin formulations were proposed by Challamel and Wang [36] to handle mixed local–nonlocal boundary conditions and to study bifurcation phenomena. For nonlinear problems, especially in buckling and post-buckling regimes, the Shooting Method has proven to be a reliable approach, offering high numerical stability and physical interpretability Shaat and Abdelkefi [37], Surmont and Coache [38]. Recently, a stress-driven nonlocal theory based on Bernoulli–Euler model is presented for size-dependent free vibrations of nanobeams with multiple edge cracks, Darban *et al.* [39].

These numerical developments confirm that while the classical analytical formulations of the nonlocal theory remain essential for model validation, the integration of advanced computational techniques is crucial for studying complex geometries, heterogeneity, and boundary interactions in nanostructures.The numerical solution of the Eringen's nonlocal beam equation requires a robust and accurate method capable of handling nonlinear second-order boundary value problems (BVPs) with boundary conditions prescribed at opposite ends of the spatial domain. As demonstrated in several recent works (Singh [40]), classical numerical approaches such as the finite-difference method (FDM) or collocation schemes often fail when applied to highly nonlinear systems, especially those involving nonlocal constitutive terms. In the case of the Eringen's beam, the governing equation contains nonlinear denominators of the form $(EI - \mu F\cos(\theta(s))) - 1(EI - \mu F\cos\theta(s)) - 1$, which can lead to local singularities and numerical instabilities when using grid-based methods.

As it is shown, there are plenty of works which focus on the elastica problem. Elastica theory plays an important role in the study of large displacements of slender rods. However, the majority of the studies are still limited to elastic material only. In Wang [41] paper, the traditional elastica theory is extended to an elastica-plastica theory. However, the buckling analysis is not fully understood, especially in the nanoscale. This paper, therefore, is devoted to the influence of the nonlocal theory on the postbuckling behavior of the nanorods. The validity of the method in this paper is confirmed by comparing with the existing work. The current results will also be useful for predicting nanorod strength and be helpful for the design of nanostructures and nanodevices related to nanorods.

The paper is divided into five sections. In Section 2, we formulate the elastica problem in the presence of a nonlocal strain in the form of a second order ordinary differential equation. We also discuss the value of the critical load which causes the loss of the stability of the structure. Section 3 presents our numerical solution using the built-in shooting method in *Wolfram Mathematica* [42], combining adaptive Runge–Kutta integration with iterative boundary-condition correction. In Section 4, we report the results and analyze the influence of the nonlocal parameter. Section 5 provides concluding remarks. In Appendix the analytical solution is provided for a local nonlinear elasticity theory.

2. The elastica problem

At first, in order to study the scale effect in the elastica problem, the nonlocal Eringen's theory was applied. Then, the numerical study of this problem was shown. Moreover, the critical load value calculations were demonstrated.

2.1 Nonlocal theory formulation

The nonlocal stress-gradient theory combines the aspects of both nonlocal elasticity and stress-gradient theories, thereby considering both the long-range interactions and the higher-order stress gradients. Within this framework, the stress state at point x is influenced by the strains at all other points in the body. In particular, the nonlocal stress-gradient theory can be reduced to both classical nonlocal elasticity theory and stress-gradient theory, hence offering a comprehensive method that encompasses both theoretical concepts. The nonlocal elasticity theory was initially formulated by Eringen [43] and Eringen and Edelen [44] by means of

integral constitutive equation. In the framework of continuum mechanics, the nonlocal elasticity theory proposed by Eringen has become a widely used approach for modeling structures in nanoscale.

The only nonzero strain of the Euler–Bernoulli beam theory, accounting for the Kirchhoff assumption, is [24]:

$$\varepsilon_{xx} = \frac{\mathrm{d}u_1}{dx} - y\frac{d^2u_2}{dx^2} = \varepsilon_{xx0} + y\kappa \tag{2.1a}$$

where $\varepsilon_{xx0} = \frac{du_1}{dx}$ are the extensional and bending strains as $y\kappa$, respectively.
Eringen's theory can be expressed either in an integral form, which explicitly accounts for long-range interactions, or in an equivalent differential form that is often more convenient for analytical and numerical treatments. In this paper, Eringen's differential form is examine and the governing equations for the nonlocal model can be written as [45]:

$$\sigma_{xx} - \mu\frac{d^2\sigma_{xx}}{dx^2} = E\varepsilon_{xx}, \tag{2.1}$$

where σ_{xx}, ε_{xx}, E and μ denotes normal stress, normal strain, Young's modulus and nonlocal parameter, respectively. The model of elastic medium based on the equation of state (2.1) and its relationship with the Eringen's nonlocal theory was also analyzed by Romano and Barretta [46], and other researchers, e.g. Nobili and Pramanik [47]. Barretta *et al.* [48] have identified a simple constitutive strategy for nanotechnological applications by differential law with a more efficient version with the contributions of Fernández-Sáez *et al.* [49]. The newly developed method is in harmony with the integral method [48]. The present work is motivated by the enhanced Eringen differential model for all boundary conditions which is developed by Barretta *et al.* [48]. It has to be nevertheless emphasized that the connection between differential and integral forms is steel an open question. The equations are based on a specific assumption about the propagator, or kernel in the integral form. Several recent works investigated various forms of propagators and the constitutive boundary conditions they imply; see, for example, Ceballes *et al.* [50], Kaplunov *et al.*[51], Pham and Vu [52], Barretta *et al.*[53], Song *et al.* [54], Pramanik and Nobili [55], Pisano *et al.* [56], Song *et al.* [57-59].

Both approaches -integral and differential- require the use of material and geometric parameters, and their clear interpretation is necessary for accurate analysis. The effect of nonlocality has been implemented to the constitutive differential equation (2.1) by the nonlocal parameter μ. The nonlocal parameter value depends on the material and the geometry of the element and it is largely determined experimentally, therefore the exact value of the nonlocal parameter μ is still not known. Here we take it as a free parameter, aiming to study its influence. Table 1 provides a literature overview of the main terms used for the nonlocal theory description. e_0 denotes material constant, a is an internal characteristic length which can represent a granular size or *a* distance between *C*-*C* bonds [60], e_0 is a characteristic magnitude of a structure, for example nanotube diameter [61].

Table 1 summarizes different ways researchers have introduced the nonlocal parameter in Eringen's nonlocal elasticity theory, highlighting the lack of a single universal definition. The

reported values vary depending on the adopted model, material characteristics, and methodological choices. Importantly, research in this field is still very active, and new studies continue to refine the interpretation and application of the nonlocal parameter to improve predictive models for advanced nanomaterials. In this study, we aim to evaluate nonlocal parameter value to contribute to the ongoing discussion and to provide further insights into its proper application and establish hypotheses for subsequent experimental validation.

Tab. 1. Various ways to introduce the nonlocal parameter.

Parameter	Symbol	Magnitude	Researcher	Material
internal characteristic length [nm]	a	0.142	Eringen [45]	carbon nanostructures
scale coefficient [-]	e_0	0.39; 0.50; 0.70	Timesli[62]	mathematical model
		0.288-0.5	Wang, Zhang [63]	carbon nanostructures
		0-1	Reddy, Pang [64]	carbon nanotubes
		0.288	Wang, Hu [65]	carbon nanostructures
		0.39	Eringen[45]	single-walled carbon nanotubes
product of nonlocal parameter and internal characteristic length [nm]	e_0a	1	Akpinar *et al.*[66]	carbon nanorods and nanotubes
		0; 2.0; 4.0	Natsuki et al. [67]	single-walled carbon nanotubes
		1	Uzun[68]	porous functionally graded nanostructures
		0; 1.0; 1.5	Ebrahimi [69]	single-walled carbon nanotubes
		0.5	Murmu[70]	single-walled carbon nanotubes
		0-1	Wang *et al.*[71]	single-walled carbon nanotubes
nonlocal parameter squared [-]	$\mu = (e_0a\ /\ l)^2$	0-1	Khaniki[72]	carbon nanorod
		0.04	Thongyothee[73]	mathematical model
nonlocal parameter [-]	$e_0a/\ h_0$	0-0.8	Karličić, Murmu [60]	multi-walled carbon nanotubes
		0-0.6	Lu [74]	multi-walled carbon nanotubes
normalized nonlocal parameter [-]	$\psi = e_0a\ /\ l$	0-0.20	De Rosa *et al.* [75]	single-walled carbon nanotubes

The standard theory for describing the buckling phenomenon is well established Euler's theory. There is a starting point of our calculations and we present it in the Appendix. In Euler's theory we describe the deflection and change in the curvature of the compressed rod due to the applied force, Equations (A.7) and (A.8) can be used to plot elasticaes to calculate the deflection and

the displacement of the end of the rod. In this work we use Eringen's theory for the deflected shape of the nanorods where the moment-curvature equation (Eq. (A.3)) is modified into [45]:

$$\frac{d\theta(s)}{ds} = -\frac{1}{EI}\left(M - \mu\frac{d^2M}{dx^2}\right), \tag{2.2}$$

where M is the bending moment at any point along the rod axis and the nonlocal part is expressed in the second derivative in momentum.

The study introduces a differential version of Eringen's nonlocal beam theory for elastic materials, constructed separately from the original integral framework. Our aim now is to solve equation (2.2) and obtain the solution that we can estimate the influence of the nonlocal parameter μ on the elasticaes shape.

The small segment shown in Figure1 is consistent with the calculations presented below and is provided for discussion. In this work, we adopt a reference frame that is more suitable for our purposes; however, we wish to emphasize that it is the reverse of the one used in Thongyothee and Chucheepsakul [24], due to adaptation to the coordinate system applied here.

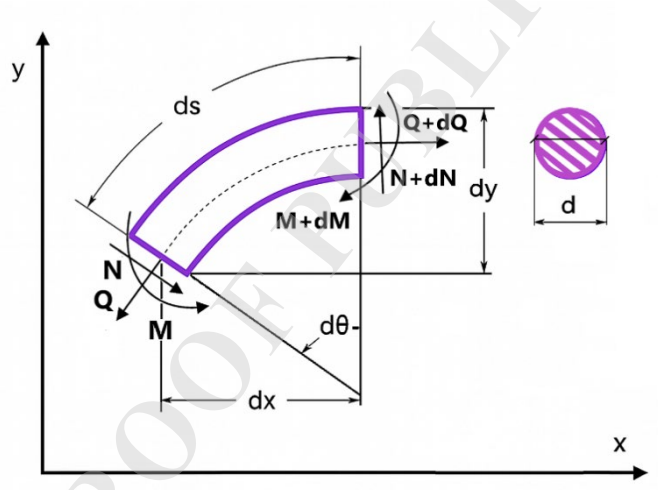

Fig. 1. The small segment of the compressed nanorod, shown in the present reference frame (based on [24]).

The equilibrium equations relating the gradients of the normal force N, shear force Q and bending moment M along the arc-length s to the curvatureκ are as follows:

$$\frac{dN}{ds} = \kappa Q, \tag{2.3}$$

$$\frac{dQ}{ds} = -\kappa N, \tag{2.4}$$

$$\frac{dM}{ds} = Q. \tag{2.5}$$

Then in Eringen's notation:

(2.6) $$\frac{dM}{dx} = \frac{dM}{ds} * \frac{ds}{dx} = \eta Q.$$

The factor $\frac{ds}{dx}$ is not defined; however, it is established that strain may be expressed in this form, namely:

(2.7) $$\sigma_{(ds)} = E\varepsilon_{(ds)},$$

where E, $\sigma_{(ds)}$ and $\varepsilon_{(ds)}$denotes Young's modulus, the normal stress and strain, respectively.

The normal strain can be measured as a difference between the current and reference configurations along the axis, and the unknown factor $\frac{ds}{dx}$ can be denoted as η:

(2.8) $$\varepsilon_{(ds)} = \frac{ds}{dx} - \frac{dx}{dx} = \eta - 1.$$

As is well known, the stress $\sigma_{(ds)}$can be expressed in terms of the axial normal force N and the cross-sectional area A as:

(2.9) $$\sigma_{(ds)} = \frac{N}{A}.$$

We can now express equation (2.7) as follows:

(2.10) $$\frac{N}{A} = E(\eta - 1),$$

(2.11) $$\eta = \frac{N}{EA} + 1.$$

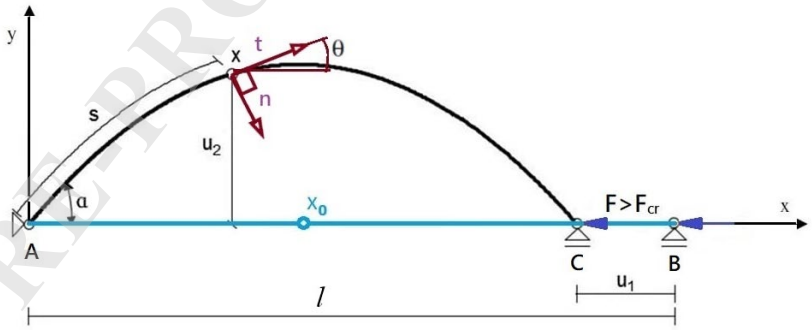

Fig. 2. Compressing of the rod due to applied force *F*.

The bending behavior is described by the bending moment M. As it is presented in Fig. 2 for the loading considered, this moment is caused by the axial force F acting at the deflection $u_2(s)$:

(2.12) $$M = Fu_2(s).$$

The corresponding shear force Q is obtained as the derivative of the bending moment with respect to the arc-length coordinate s. Making use of the kinematic relation between the deflection and the rotation angle of the cross-section $\theta(s)$, this leads to:

$$Q = \frac{dM}{ds} = d\frac{Fu_2(s)}{ds} = F\sin\theta(s). \tag{2.13}$$

We can now express equation (2.3) as follows:

$$N = \frac{-1}{\frac{d\theta(s)}{ds}} * \frac{dQ}{ds} = \frac{-1}{\frac{d\theta(s)}{ds}} * \frac{d}{ds}\left(F\sin\theta(s)\right) = \frac{-1}{\frac{d\theta(s)}{ds}} * F\cos\theta(s)\frac{d\theta(s)}{ds} = -F\cos\theta(s). \tag{2.14}$$

We can express η as:

$$\eta = \frac{N}{EA} + 1 = -\frac{F\cos\theta(s)}{EA} + 1. \tag{2.15}$$

Then:

$$\frac{dM}{dx} = \frac{dM}{ds} * \frac{ds}{dx} = \eta Q = \left(\frac{N}{EA} + 1\right) * Q. \tag{2.16}$$

Then we can obtain:

$$\frac{d^2M}{dx^2} = \frac{d}{dx}\left(\frac{QN}{EA} + Q\right) = \frac{1}{EA}\frac{d}{dx}(QN) + \frac{dQ}{dx} = \frac{1}{EA}\left(\frac{dQ}{dx} * N + \frac{dN}{dx} * Q\right) + \frac{dQ}{dx}. \tag{2.17}$$

Subsequently, the derivatives are determined:

$$\frac{dQ}{dx} = \frac{dQ}{ds} * \eta = -\kappa\eta N, \tag{2.18}$$

$$\frac{dN}{dx} = \frac{dN}{dx} * \eta = \kappa\eta Q. \tag{2.19}$$

Then using (2.18) and (2.19) we obtain:

$$\frac{d^2M}{dx^2} = \frac{1}{EA}(-\kappa\eta N^2 + \kappa\eta Q^2) - \kappa\eta N = \frac{1}{EA}\left(\kappa\eta(Q^2 - N^2)\right) - \kappa\eta N. \tag{2.20}$$

Then using (2.2) we obtain:

$$\frac{d\theta(s)}{ds} = -\frac{1}{EI}\left(M - \mu\left(\frac{1}{EA}\left(\frac{d\theta(s)}{ds}\eta(Q^2 - N^2)\right) - \frac{d\theta(s)}{ds}\eta N\right)\right), \tag{2.21}$$

(2.22) $$\frac{d\theta(s)}{ds}\left(1-\frac{\mu}{EIEA}\eta(Q^2-N^2)+\frac{\eta\mu N}{EI}\right)=-\frac{M}{EI},$$

(2.23) $$\frac{d\theta(s)}{ds}=-\frac{M}{EI}*\left(\frac{1}{1-\frac{\mu\,\eta}{EIEA}(Q^2-N^2)+\frac{\eta\mu N}{EI}}\right),$$

this is identical to that given by [24].

Now we are looking for the second derivative θ of the variables:

(2.24) $$\frac{d^2\theta}{ds^2}=-\frac{1}{EI}\frac{d}{ds}\left(\frac{M}{1-\frac{\mu\,\eta}{EIEA}(Q^2-N^2)+\frac{\eta\mu N}{EI}}\right).$$

(2.25) $$\frac{d^2\theta}{ds^2}=$$
$$-\frac{1}{EI}\frac{d}{ds}\left(\frac{Fu_2(s)}{1-\frac{\mu}{EIEA}\left(F^2-\frac{F^3\cos\theta(s)}{EA}+\frac{2F^3\cos^3\theta(s)}{EA}-2F^2cos^2\theta(s)\right)+\left(\frac{\mu F^2\cos^2\theta(s)}{EIEA}-\frac{\mu F\cos\theta(s)}{EI}\right)}\right),$$

(2.26) $$\frac{d^2\theta}{ds^2}=$$
$$-\frac{1}{EI}\frac{d}{ds}\left(\frac{Fu_2(s)}{1-\frac{\mu F^2}{EIEA}+\frac{\mu F^3\cos\theta(s)}{EIEAEA}-\frac{2\mu F^3\cos^3\theta(s)}{EIEAEA}+\frac{3\mu F^2\cos^2\theta(s)}{EIEA}-\frac{\mu F\cos\theta(s)}{EI}}\right).$$

To the best of our knowledge, this Eq. (2.26) with second derivative has not been presented in the literature. It is worth to mention that in Eringen's theory for $\mu=0$ we obtain the classical Euler's theory (Eq. (A2.p).

2.2 Critical load value

According to Euler's theory we can calculate the critical load which causes the loss of the stability of the structure using the following formula [76]:

(2.27) $$P_{crE}=EI\left(\frac{\pi n}{l}\right)^2,$$

where $n=0,1,3\ldots$

From the engineering point of view it is very useful to apply this formula to obtain a discrete set of values of the load for a particular material to prevent buckling phenomena. However, in nonlinear elasticity theory the critical load value is not a constant and depends on the elliptic

integral of the first kind $K(k)$, related with the initial angle $\alpha = \theta(0)$. We can calculate it using Bigoni's formula [77]:

(2.28)
$$P_{cr} = EI\left(\frac{m}{l}\right)^2\left[2K\left(sin\frac{\alpha}{2}\right)\right]^2.$$

This formula (2.28) is going to be used in Section 3 in order to estimate the reference axial force value.

3. Numerical solution of the elastica problem

3.1 Method

In this Section we adopt the shooting method, as implemented in Wolfram Mathematica [42], to obtain the solution of the second-order nonlinear differential equation governing the nonlocal Eringen's beam (Eq. (2.26)). This approach converts a boundary value problem (BVP) into an equivalent initial value problem (IVP), which is iteratively solved until the boundary conditions at both ends of the beam are satisfied.

The shooting method was chosen because of its numerical stability and robustness when dealing with nonlinear differential equations containing trigonometric terms and variable coefficients in the denominator, such as in the Eringen's model. Alternative approaches, such as the finite difference or collocation methods, often lead to convergence issues near points where the denominator in Eg. (2.26) becomes small. In contrast, the shooting method allows direct control over the boundary conditions and provides stable convergence even for strongly nonlinear systems, as such.

In the numerical implementation, the built-in solver *NDSolve* was used with the option: Method → "Shooting". This solver internally applies an adaptive Runge–Kutta algorithm with variable order (Dormand–Prince/Fehlberg type). The algorithm automatically adjusts both the integration step and the order according to the local truncation error, ensuring high accuracy while maintaining computational efficiency.

3.2 Implementation details

The final algorithm was implemented as a boundary value problem (BVP) solved by the built-in *Shooting Method* in Wolfram Mathematica [42]. The governing system consisted of three first-order differential equations:

(2.29)
$$\theta'(s) = \kappa(s),$$

(2.30)
$$\kappa'(s) = -\frac{F}{EI - \mu F\cos\theta(s)}\sin\theta(s),$$

(2.31)
$$u_2'(s) = \sin\theta(s),$$

with mixed Dirichlet–von Neumann clamped–pinned boundary conditions:

(2.32)
$$\theta(s=0)=\alpha,$$

(2.33)
$$\theta'(s=l)=0,$$

(2.34)
$$u_2'(s=l)=0.$$

This boundary conditions are motivated by recent experiment on nanorods, recently published by Manecka-Padaż [78]. The algorithm treats the initial curvature $\kappa(0)$as a *shooting parameter*. For a guessed value of $\kappa(0)$, the system is integrated from $s=0$ to $s=l$ using an adaptive Runge–Kutta scheme (Dormand–Prince type [79, 80]). After each integration, two residuals are evaluated:

(2.35)
$$R_1=\theta'\big(l;\kappa(0)\big),$$

(2.36)
$$R_2=u_2'\big(l;\kappa(0)\big).$$

The initial slope $\kappa(0)$is then iteratively corrected using a secant or Newton-type update until both residuals satisfy the prescribed tolerance ($|R_1|,|R_2|<10^{-6}$).

This procedure ensures that the end of the beam satisfies both mechanical and geometric constraints simultaneously. The adaptive step-size control built into the solver prevents numerical instabilities near regions where $EI-\mu F\cos\theta(s)$approaches zero, ensuring smooth convergence even for relatively large nonlocal parameters μ. The critical value μ_{cr} is decreasing with increasing value of initial angle $\alpha=\theta(0)$.This hybrid approach combines the accuracy of adaptive integration with the flexibility of iterative boundary correction, offering excellent numerical stability and control of the solution error. Moreover, the adaptive step-size control allowed the solver to handle regions with steep curvature gradients or strong geometric nonlinearity without loss of accuracy.

The choice of the shooting method is also justified from a physical standpoint. Unlike mesh-based numerical techniques, which require additional artificial constraints, the shooting method directly mirrors the physical process of "matching" the beam shape to the boundary conditions. This makes it particularly suitable for bifurcation-type problems and for analysing stability modes of nanobeams.

3.3 Model Parameters and Reference Force

In the numerical simulations, the material and geometric parameters were chosen to represent a slender nanobeam of length $l=1000$ nm. The selected values correspond to realistic mechanical properties of nanostructures such as silicon nanobridges or carbon nanotubes and are consistent with earlier studies based on the Euler–Bernoulli beam model.

Numerical simulations were performed for a normalized beam model with the parameters $l=1000$ nm and $EI=EA=1$, m=1 and $\mu\in\{0;\ 0{,}01;\ 0{,}02,\ 0{,}03;\ 0{,}04;\ 0{,}05\}$. The parameters EI and EA were selected to ensure compatibility with the local Euler–Bernoulli model in the

limit $\mu \to 0$, allowing direct comparison between classical and nonlocal solutions. To provide a consistent basis for comparison between local and nonlocal models, the reference axial force F was used according Eq. (2.28), mentioned in Section 2.3. Employing Euler's critical force as the reference value ensures both physical and numerical consistency between the local and nonlocal formulations. This choice allows a direct evaluation of how the nonlocal parameter μ modifies the effective stiffness and the beam curvature distribution. As μ decreases, the computed results reveal a clear *structural softening effect;* the deformation becomes smoother, and the effective rigidity $EI_{\text{eff}} = EI - \mu F \cos\theta(s)$ decreases, confirming the expected nonlocal influence predicted by Eringen's theory.

The values of *EI* and *EA* for a circular cross-section (as in Fig. 1) can be calculated using the formulas:

(2.37)
$$EI = \frac{E\pi d^4}{64},$$

(2.38)
$$EA = \frac{E\pi d^2}{4}.$$

4. Results

The numerical results obtained with this method showed good agreement with the classical Euler–Bernoulli solutions for $\mu = 0$, and for increasing values of the nonlocal parameter μ, a clear structural softening effect was observed. This effect manifests as a reduction of the effective stiffness and a smoother distribution of curvature along the beam length, confirming the expected influence of nonlocality in the Eringen's framework. The resulting solution $\theta(s)$and $u_2'(s)$was subsequently used to reconstruct the beam profile $y(x)$.

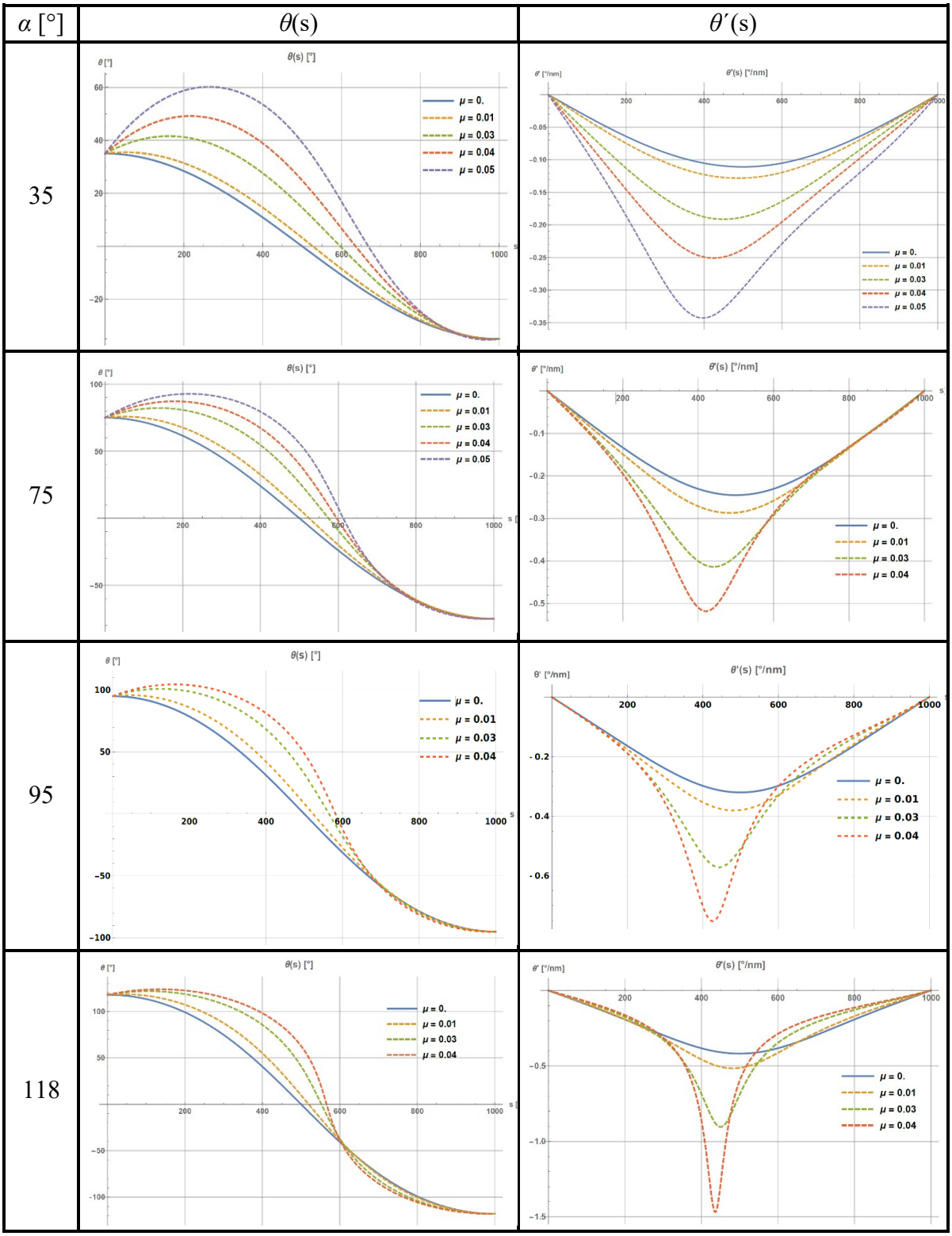

Fig. 3. Set of bending angles θ and their derivatives as a function of a coordinate along the rod s. We present four pairs for four different initial angles $\alpha = \theta(0)$. On each panel values for different nonlocal parameter μ are shown.

In Fig. 3 we see that as the nonlocal parameter μ increases, the angle θ increases along the curvilinear coordinate s. For an equal increment in μ, this change becomes more pronounced at higher values - there is a smaller difference in θ between $\mu = 0.01$ and $\mu = 0.03$ than between $\mu = 0.03$ and $\mu = 0.05$. With an increasing initial angle $\alpha = \theta(0)$, this effect becomes less

evident, and the θ profile becomes more slender. For larger α (i.e., $\alpha = 95°$ and 118°), the trend reverses: a critical point appears (the larger α, the earlier it occurs), beyond which θ falls below the prediction of the local theory as s varies. In the θ' plot, the influence of μ on the rod's curvature is substantial, and it intensifies with increasing initial angle α. Further quantitative analysis of results shown in Fig. 3 is presented in Table 2. To satisfy the boundary conditions, it was necessary to assume an extension of the nanorod δl. For each μ we give the necessary change of length of the beam δl. We see that δl increases with μ and is the largest for the smallest initial angles α.

Tab. 2. Quantitative analysis of the results in Fig. 3.

α	**35°**		**75°**		**95°**		**118°**	
μ	Δl [nm]	Δl/l %	Δl [nm]	Δl/l %	Δl [nm]	Δl/l %	Δl [nm]	Δl/l %
0.01	49.71	4.97	46.80	4.68	43.85	4.39	37.87	3.79
0.03	144.64	14.46	128.81	12.88	118.45	11.85	101.40	10.14
0.04	183.35	18.34	163.45	16.35	150.79	15.08	129.75	12.98

As it is presented in Fig. 4 the shape of the elastic $y(x)$ also changes noticeably under the nonlocal theory. A softening of the compressed rod is evident – the larger the nonlocal parameter μ, the more compliant the rod becomes to shape change. The curves obtained under the nonlocal theory resemble those corresponding to higher angles in the local theory (e.g., for α = 95°, and disregarding the boundary condition, the deformation pattern is similar to that in the local theory for 120°).

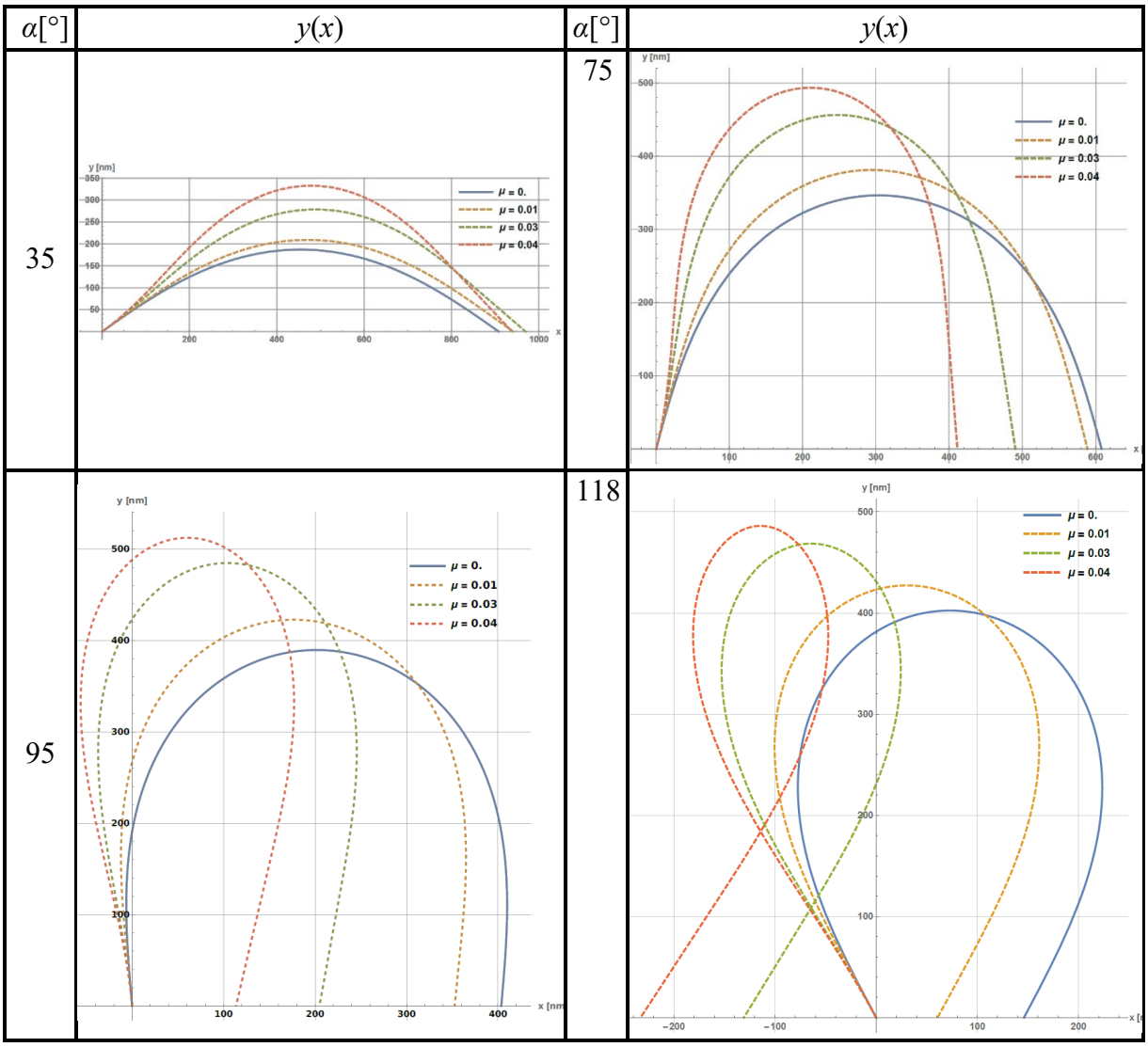

Fig. 4.The influence of the nonlocal theory on the shape of the elasticaes for the given values of the initial angle α.

Further quantitative analysis of the maxima's position is presented in Table 3. It can be observed that the nonlocal theory implies an earlier onset of deformation with a broadly similar overall form (though not identical, as evidenced by the left-side inflection of the rod). The maximum deflection does not occur at midspan (the problem becomes asymmetric, in contrast to the local formulation), and this tendency is most prominent for small initial angles. This is analyzed in detail in Table 3 where it can be seen that maximum is shifted from the mid-span ($s = 500$ nm) to higher values of s. Moreover, we observe small left-hand-side inflection and it is more visible for smaller values of the initial angle and for higher μ. For each initial angle we have extracted also a critical value of the nonlocal parameter μ_{cr} (down row in Tab. 3) where the theory on our level of approximation breaks down. This is because the dominator in Eq. (2.26) approaches zero. The values of μ_{cr} decreases with the increasing initial angle α.

Tab. 3. Quantitative analysis of the maxima's position and critical value of nonlocal parameter μ_{cr}.

α	35°			75°			95°			118°		
μ	$x_{\max}$	$y_{\max}$	$s_{\max}$	$x_{\max}$	$y_{\max}$	$s_{\max}$	$x_{\max}$	$y_{\max}$	$s_{\max}$	$x_{\max}$	$y_{\max}$	$s_{\max}$
0.00	454.3	186.9	500.0	304.0	346.3	500.0	201.8	389.503	500.0	73.04	402.4	500.0
0.01	471.0	209.1	525.0	294.6	381.1	523.5	176.5	422.697	522.0	30.3	427.3	518.8
0.03	488.9	278.7	575.3	247.6	456.3	564.8	104.3	484.667	559.0	-64.1	468.5	550.2
0.04	478.6	332.6	598.3	210.5	493.4	582.3	60.3	512.3	574.57	-114.2	486.1	563.7
μ_{cr}	**0.0967**			**0.0809**			**0.06978**			**0.0551**		

5. Conclusions

There are two main results that we obtained in this work. Firstly, we have derived the nonlocal constitutive laws for Eringen's theory. They are equations for the derivative of the beam's curvature and their form is very similar to that of a classical Euler's elastica. This allows for an immediate comparison of the two theories. One observes that the nonlocality appears in the denominator, which in principle may lead to instability. The second main result is that we have solved these equations numerically using the shooting method. That finding a new numerical method is here a valuable outcome by itself is witnessed by a very well cited paper by Omer Civalek *et al.* [81] where a new differential quadrature method was proposed to solve a very similar nonlocal problem.

The computed results reveal a clear structural softening effect – the deformation becomes smoother, and the effective rigidity $EI_{eff} = EI - \mu F\cos\theta(s)$ decreases, confirming the expected nonlocal influence predicted by Eringen's theory. We applied mixed boundary conditions on both ends which corresponds to physical situation such as the way experiments on nanorods are performed. Interestingly, while the Euler's elastica shows symmetric bending, within the Eringen's theory there is clear anisotropy: the maximum curvature is shifted towards left side of the beam. This effect can be considered as a hallmark of the presence of nonlocal elasticity when the beams are measured experimentally.

Increasing nonlocality parameter μ and initial angleα brings the system closer to the instability which manifest as a singular behavior of curvature's derivative. Further extension of the theory will be needed to mitigate this effect. If one considers that elastica theory is an effective continuum description that emerges upon averaging microscopic degrees of freedom then one may suspect that including anharmonicity of underlying lattice will prevent an appearance of too strong local curvature.

Eringen's theory remains the subject of ongoing debate, particularly with respect to its differential formulation. The specific values of the nonlocal parameter μ, which directly accounts for nonlocality in a given structure, are also not yet well established. Since the problem has not been fully explored, a promising direction for the Author's future work will be the implementation of constitutive boundary conditions, especially in studies that incorporate experimental results for a specific material. As described in Subsec. 2.1, the constitutive boundary conditions are mathematically derived, for a given propagator, and they allow to build a connection between differential and integral formulation of the theory. It is not obvious what is their relation with the physically observed boundary conditions, in the future one could add

constitutive BC as a part of the shooting optimization procedure and/or investigate what propagators are imposed by a given physical setting. We believe these are fascinating future directions for research of nonlocality in nanostructures.

Appendix

Euler's formula

We consider a simply supported elastic inextensible circular rod of the length l subjected to the compressive load F applied at point B, as shown in Fig. 2. During compression the rod changes its curvature and we can note α as an initial angle at point A, u_1 is the displacement of the end of the rod in the right support from point B to C, u_2 is the deflection at point X, $\boldsymbol{t}$ and $\boldsymbol{n}$ are tangent and normal vectors in X, respectively.

The governing differential equation for the elastica can be expressed as [45]:

$$\theta(s)'' + \lambda^2 \sin\theta(s) = 0, \tag{A.1}$$

Where θ is the angle of inclination of the tangent $\boldsymbol{t}$ to the elastica at point X, $\lambda^2 = \frac{F}{EI}$, F is axially applied load, E is Young's modulus, I is the moment of inertia and $s$is the nondimensional arclength defined by its centerline and $s \in [0, l]$.

Also in basic geometry considerations relating to the displacement vector starts at point X_0 and ends in X we obtain the standard relation between curvature and the rotation angle of the tangent:

$$\varkappa = \frac{d\theta}{ds}. \tag{A.2}$$

The moment-curvature relationship can be expressed as [67]:

$$\varkappa = \frac{d\theta}{ds} = \frac{M}{EI}. \tag{A.3}$$

The boundary conditions for simply supported beam are:

$$u_1(0) = 0, \tag{A.4}$$

$$u_2(0) = u_2(l) = 0, \tag{A.5}$$

$$\theta'(0) = \theta'(l) = 0. \tag{A.6}$$

These boundary conditions describe the theoretical framework of the classical Euler's buckling case, in which a slender elastic rod is subjected to axial compression between two hinged supports. In this formulation, the supports prevent transverse displacements while permitting free rotations, thereby providing a coherent mathematical representation of the problem. In our approach, we aim to obtain the elastica shape for a given initial angle and bifurcation mode m. In this case, the system of equations describing the elastica determines for each chosen point X along the rod axis the corresponding coordinates x and y.

Taking into account the boundary conditions (Eqs. (A.4), (A.5) and (A.6)) and using elliptic integrals we can solve the governing Eq. (2.1) obtaining the solution, equal to presented in [77]:

(A.7) $$x = -s + \frac{2}{\lambda}\{E[am(s\lambda + K(k), k), k] - E[am(K(k), k), k]\},$$

(A.8) $$y = -\frac{2k}{\lambda} cn(s\lambda + K(k), k),$$

where x, y are coordinates on the rod axes and $x, y \in < 0, l >$, $x_1, x_2 \in < 0, l >$, $E(k)$ is the incomplete elliptic integral of the second kind and $E(x,k) = \int_0^x \sqrt{1 - k sin^2 t} dt$, $k = sin\frac{\alpha}{2}$, α is the initial angle and $\alpha = \theta(0)$ and $0 \leq \alpha \leq \pi$, $K(k)$is the complete elliptic integral of the first kind and $K(k) = \int_0^{\frac{\pi}{2}} \frac{d\phi}{\sqrt{1-k^2 sin^2 \phi}}$.

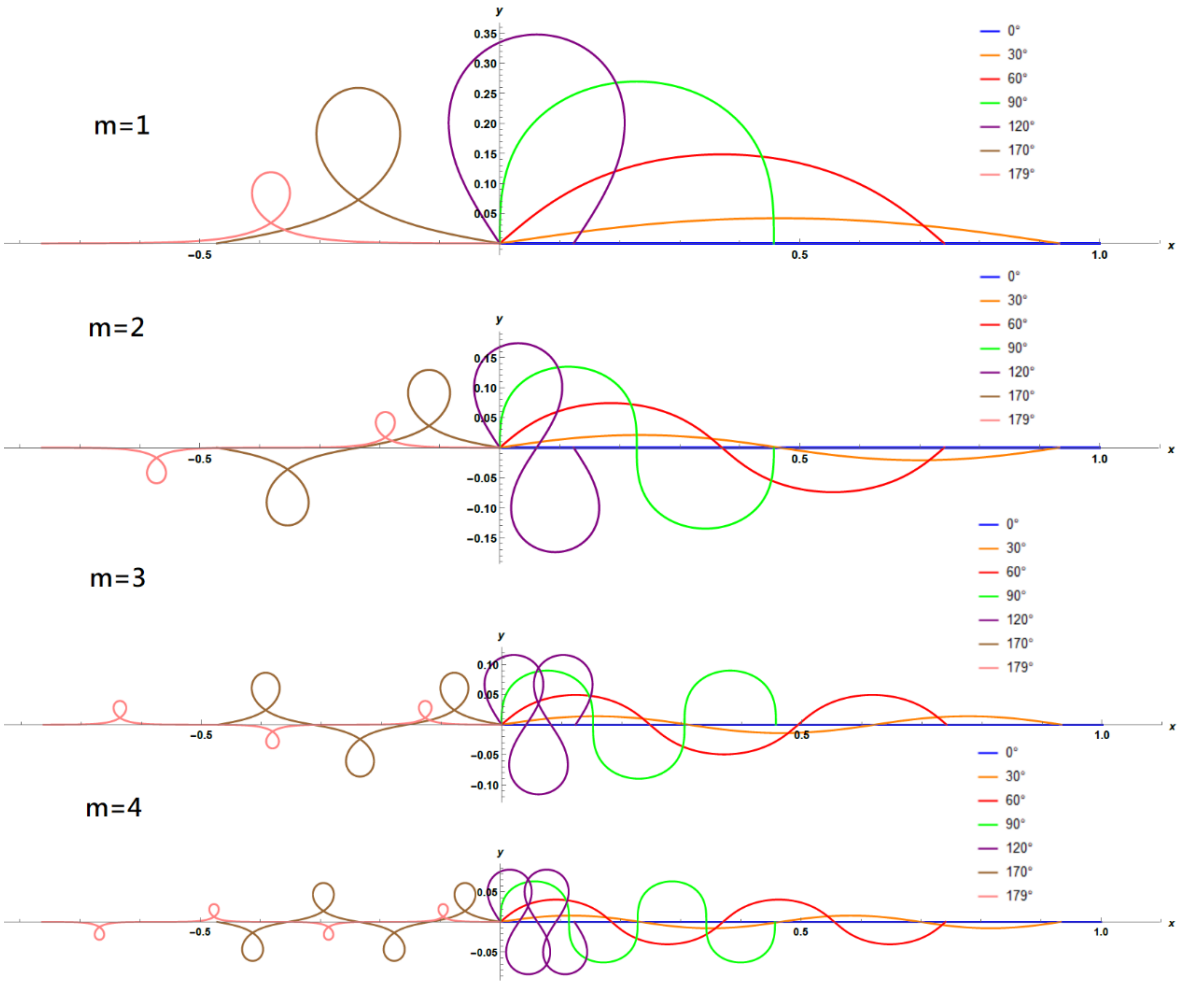

Fig. 5. Various shapes of elastica for given initial angle α and m-th mode of the bifurcation.

Using Eqs. (A.7) and (A.8) the solution for a given initial angle α and mode m can be plotted. In Fig. 5 the elasticaes lines are shown for various values of the initial angle ($\alpha = 30°, 60°, 90°, 120°, 170°$ and $179°$) and or the m-th mode of the bifurcation ($m = 1, 2, 3$ and 4). It is a representation of the postcritical behavior of the compressed rod. Figure 2 visualizes how the nonlinear postbuckling shapes evolve with different bifurcation modes m. Higher m leads to more complex deflection patterns and richer branches of solutions.

First mode ($m = 1$) is the most critical case, because it occurs at the lowest load and produces the largest mid-span deflection. In second mode ($m = 2$) the rod bends into two half-waves, with a node at the midpoint. The mid-span deflection is approximately half of that in mode $m = 1$ and occurs symmetrically upward and downward along the axis. It needs a 4 times higher critical load value than in the first mode. In the third mode ($m = 3$) the rod exhibits three half-waves, with two interior nodes. The mid-span deflection is around three times smaller than $m = 1$ for a nine times higher critical load value. In the fourth mode ($m = 4$) the rod deforms into four half-waves, with three interior nodes. The maximum deflection is about one-quarter of that in mode $m = 1$, while requiring a sixteen-fold higher critical load. The inherent symmetry of the problem is clearly reflected in these deformation shapes.

These particular initial angles (0°, 30°, 60°, 90°, 120°, 170°, 179°) were selected to illustrate the full spectrum of elastica behavior. For small angles (0°–30°), the rod shows relatively gentle deflections with smooth, gradually increasing curvature. Medium angles (60°–120°) highlight the stronger nonlinear character of the elastica, with curves bending more significantly and beginning to form loops, particularly in higher buckling cases. Very large angles (170°–179°) correspond to extreme cases, where the rod shape approaches self-intersecting loops and folding. Because of its expected relevance to a future experiment, the analysis concentrates mainly on the first buckling mode.

References

1. Zaccaria D., Bigoni D., Noselli G., Misseroni D., Structures buckling under tensile dead load, *Proceedings of the Royal Society A*, **467**(2130): 1686-1700, 2011, https://doi.10.1098/rspa.2010.0505.
2. Bistafa S.R., Euler's Variational Approach to the Elastica, *Euleriana*, **3**(2): 156-175, 2023, https://doi.org/10.48550/arXiv.2303.18126.
3. Shigeki M., Euler's Elastica and Beyond, *J. Geom. Symmetry Phys.*, **17**: 45-86, 2010, https://doi.org/10.7546/jgsp-17-2010-45-86.
4. Kirchhoff G., Über das Gleichgewicht und die Bewegung einer elastischen Scheibe, *Journal für die reine und angewandte Mathematik*, **40**: 5-88, 1850, http://eudml.org/doc/147439.
5. Born M., *Untersuchungen über die stabilität der elastischen Linie in Ebene und Raum: Unter verschiedenen Grenzbedingungen,* Vandenhoeck and Ruprecht, 1906.
6. Nishinari K., Nonlinear dynamics of solitary waves in an extensible rod, *Proc. R. Soc. Lond. A.*, **453**: 817-833, 1997, https://doi.org/10.1098/rspa.1997.0045.
7. Chucheepsakul S., Monprapussorn T., Divergence Instability of Variable-Arc-Length Elastica Pipes Transporting Fluid, *Journal of Fluids and Structures*, **14**: 895-916, 2000, https://doi.org/10.1006/jfls.2000.0301.
8. Vassilev V.M., Djondjorov P.A., Mladenov I.M., Cylindrical equilibrium shapes of fluid membranes, *Journal of Physics A: Mathematical and Theoretical*, **41**: 435201, 2008, https://doi.org/10.48550/arXiv.0803.0843.
9. Kibach H., Ture Savadkoohi A., Lamarque C.-H., Free vibrations of an elastica around its post-buckled configurations, *International Journal of Non-Linear Mechanics*, **179**: 105250, 2025, https://doi.org/10.1016/j.ijnonlinmec.2025.105250.

10. Taloni A., Vilone D., Ruta G., General theory for plane extensible elastica with arbitrary undeformed shape, *International Journal of Engineering Science*, **193**: 103941, 2023, https://doi.org/10.1016/j.ijengsci.2023.103941.
11. Leanza S., Zhao R.R., Hutchinson J.W., The elastica with pre-stress due to natural curvature, *Journal of the Mechanics and Physics of Solids*, **190**: 105690, 2024, https://doi.org/10.1016/j.jmps.2024.105690.
12. Phungpaingam B. and Chucheepsakul S., Postbuckling behavior of variable-arc-length elastica connected with a rotational spring joint including the effect of configurational force, *Meccanica*, **53**(10): 2619-2636, 2018, https://doi.10.1007/s11012-018-0847-x.
13. Lai B., Liew J.Y.R., Wang T., Buckling behaviour of high strength concrete encased steel composite columns, *Journal of Constructional Steel Research*, **154**: 27-42, 2019, https://doi.10.1016/j.jcsr.2018.11.023.
14. Wang Q., Zou H. L., Deng Z.C., Snap-through of an elastica under bilateral displacement control at a material point, *Acta Mechanica Sinica/Lixue Xuebao*, **36**(3): 727-734, 2020, https://doi.10.1007/s10409-020-00937-4.
15. Fraldi M., Palumbo S., Cutolo A., Carotenuto A.R., Bigoni D., Bimodal buckling governs human fingers' luxation, *Proceedings of the National Academy of Sciences of the United States of America*, **120**(44): e2311637120 , 2023, https://doi.10.1073/pnas.2311637120.
16. Hathaipichitchai P., Klaycham K., Jiammeepreecha W., Athisakul C., Chucheepsakul S., Postbuckling behavior of variable-arc-length elastica pipe conveying fluid including effects of self-weight and pressure variation, *International Journal of Non-Linear Mechanics*, **164**: 104760, 2024, https://doi.10.1016/j.ijnonlinmec.2024.104760.
17. Curatolo M., Napoli G., Nardinocchi P., Turzi S., Swelling-driven soft elastic catapults, *International Journal of Non-Linear Mechanics*, **162**: 104727, 2024, https://doi.10.1016/j.ijnonlinmec.2024.104727.
18. Wang X., Qiu X., Elastica-plastica theory of Euler-Bernoulli beams subjected to concentrated loads, *Applied Mathematical Modelling*, **136:** 115623, 2024, https://doi.10.1016/j.apm.2024.07.030.
19. Matsutani S., Statistical mechanics of elastica for the shape of supercoiled DNA: Hyperelliptic elastica of genus three, *Physica A: Statistical Mechanics and its Applications*, **643**: 129799, 2024, https://doi.10.1016/j.physa.2024.129799.
20. Duan H. L., Wang J., Karihaloo B. L., Theory of Elasticity at the Nanoscale, *Advances in Applied Mechanics*, **42**: 1-68, Academic Press Inc., 2009, https://doi.10.1016/S0065-2156(08)00001-X
21. Wang G. F., Feng X.Q., Surface effects on buckling of nanowires under uniaxial compression, *Applied Physics Letters*, **94(**141913): 1-3, 2009, https://doi.10.1063/1.3117505.
22. Moradi M., Fereidon A.H., S. Sadeghzadeh, Dynamic modeling for nanomanipulation of polystyrene nanorod by atomic force microscope, *Scientia Iranica*, **18(3):** 808-815, 2011, https://doi.10.1016/j.scient.2011.06.003.
23. J. L. Liu, Y. Mei, R. Xia, and W. L. Zhu, Large displacement of a static bending nanowire with surface effects, *Physica E: Low-Dimensional Systems and Nanostructures*, **44**(10): 2050-2055, 2012, doi: 10.1016/j.physe.2012.06.009.

24. Thongyothee C., Chucheepsakul S., Postbuckling of unknown-length nanobeam considering the effects of nonlocal elasticity and surface stress, *International Journal of Applied Mechanics*, **7**(3): 1550042, 2015, https://doi.10.1142/S1758825115500428.
25. Challamel N., Kocsis A., Wang C.M., Discrete and nonlocal elastica, *International Journal of Non-Linear Mechanics*, **77**: 128-140, 2015, https://doi.10.1016/j.ijnonlinmec.2015.06.012.
26. Lembo M., Exact solutions for postbuckling deformations of nanorods, *Acta Mechanica*, **228**(6): 2283-2298, 2017, https://doi.10.1007/s00707-017-1834-3.
27. Tang Y., Qing H., Bending, buckling and free vibration of Timoshenko beam-based plane frame via FEM with nonlocal integral model, *Journal of Mechanics of Materials and Structures*, **18**(3): 355-374, 2023, https://doi.10.2140/jomms.2023.18.355.
28. Hussain M., Naeem M.N., *Vibration Characteristics of Single-Walled Carbon Nanotubes Based on Nonlocal Elasticity Theory Using Wave Propagation Approach (WPA) Including Chirality*, https://www.intechopen.com/chapters/66883 (access: 2024.10.12).
29. Berecki D., Glavardanov V.B., Grahovac N.M., Zigic M.M., Bifurcation analysis of a nanotube through which passes a nanostring, *Acta Mechanica*, **235**: 6867-6888, 2024, https://doi.10.1007/s00707-024-04076-w.
30. Darban H., Fabbrocino F., Feo L., Luciano R., Size-dependent buckling analysis of nanobeams resting on two-parameter elastic foundation through stress-driven nonlocal elasticity model, *Mechanics of Advanced Materials and Structures*, **28**(23): 2021, https://doi.org/10.1080/15376494.2020.1739357.
31. Darban H., Luciano R., Darban R., Buckling of cracked micro- and nanocantilevers, *Acta Mechanica*, **234**(2): 693-704, 2023, https://doi.10.1007/s00707-022-03417-x.
32. Darban H., Elastostatics of nonuniform miniaturized beams: Explicit solutions through a nonlocal transfer matrix formulation, *International Journal of Engineering Science*, **198**: 104054, 2024, https://doi.10.1016/j.ijengsci.2024.104054.
33. Reddy J. N., Nonlocal theories for bending, buckling and vibration of beams, *International Journal of Engineering Science*, **45**(2-8): 288-307, 2007.
34. Phadikar J., Pradhan S., Variational formulation and finite element analysis for nonlocal elastic nanobeams and nanoplate,. *Computational Materials Science*, **49**(2): 492–499, 2010. https://doi.org/10.1016/j.commatsci.2010.05.040.
35. Aydogdu M., A general nonlocal beam theory: numerical solutions via differential quadrature method, Composite Structures, **89**: 275-283, 2009.
36. Challamel N., Wang C.M., On the variational formulation of nonlocal elasticity: Application to the Eringen beam, *International Journal of Solids and Structures*, **51**(23-24), 4324-4333, 2014.
37. Shaat M., Abdelkefi A., Nonlinear buckling and postbuckling of nanobeams using the shooting method within the nonlocal elasticity framework, *International Journal of Mechanical Sciences*, **124-125**, 162-175, 2017.
38. Surmont C., Coache A., Geometrically exact static 3D Cosserat rods problem solved using a shooting method, *International Journal of Non-Linear Mechanics*, **119**: 103330, 2020,https://doi.org/10.48550/arXiv.2412.09146.

39. Darban, H., Luciano R., Basista M., Free transverse vibrations of nanobeams with multiple cracks,*International Journal of Engineering Science*, **177**: 103703, 2022. https://doi.org/10.1016/j.ijengsci.2022.103703.
40. Singh J., Shooting method for solving two-point boundary value problems in ODEs numerically,[in]: *Artificial Intelligence Technology in Healthcare* , CRC Press., 2024, https://doi.org/10.48550/arXiv.2208.13221.
41. Wang X., Qiu X., Elastica-plastica theory of Euler-Bernoulli beams subjected to concentrated loads, *Applied Mathematical Modelling*, **136**: 115623, 2024, https://doi.org/10.1016/j.apm.2024.07.030.
42. *Wolfram Mathematica*, Version 14.0, Champaign, IL, USA: Wolfram Research, Inc., 2024, https://www.wolfram.com/mathematica.
43. Eringen A.C., Linear theory of nonlocal elasticity and dispersion of plane waves, *Int. J. Eng. Sci.*, **10:** 425-435, 1972, https://doi.org/10.1016/0020-7225(72)90050-X.
44. Eringen A.C., Edelen D.G.B., On nonlocal elasticity, *International Journal of Engineering Science*, **10**(3): 233-248, 1972, https://doi.org/10.1016/0020-7225(72)90039-0.
45. Eringen A.C., On differential equations of nonlocal elasticity and solutions of screw dislocation and surface waves, *J. Appl. Phys*., **54**(9): 4703-4710, 1983, https://doi.org/10.1063/1.332803.
46. Romano G., Barretta R., Nonlocal elasticity in nanobeams: the stress-driven integral model, *International Journal of Engineering Science*, **115**:14-27, 2017, https://doi.org/10.1016/j.ijengsci.2017.03.002.
47. Nobili A., Pramanik D., A well-posed theory of linear nonlocal elasticity, *International Journal of Engineering Science*, **215**: 104314, 2025, https://doi.org/10.1016/j.ijengsci.2025.104314.
48. Barretta R., Feo L., Luciano R., Marotti de Sciarra F., Application of an enhanced version of the Eringen differential model to nanotechnology, *Composites Part B: Engineering*, **96**:274-280, 2016, https://doi.org/10.1016/j.compositesb.2016.04.023.
49. Fernández-Sáez J. , Zaera R. , Loya J.A., Reddy J.N., Bending of Euler–Bernoulli beams using Eringen's integral formulation: A paradox resolved, *International Journal of Engineering Science*, **99**: 107-116, 2016, https://doi.org/10.1016/j.ijengsci.2015.10.013.
50. Ceballes S., Larkin K., Rojas E., Ghaffari S.S., Abdelkefi A., Nonlocal elasticity and boundary condition paradoxes: a review. *J. Nanoparticle Res*., **23**: 66, 2021. https://doi.org/10.1007/s11051-020-05107-y.
51. Kaplunov J., Prikazchikov D.A., Prikazchikova L., On integral and differential formulations in nonlocal elasticity, *Euro. J. Mech. A/Solids*, **100**: 104497, 2023, https://doi.org/10.1016/j.euromechsol.2021.104497
52. Pham C.V., Vu T.N.A., On the well-posedness of Eringen's non-local elasticity for harmonic plane wave problems, *Proc. R. Soc. A*, **480**: 20230814, 2024, https://doi.org/10.1098/rspa.2023.0814
53. Barretta R., Luciano R., de Sciarra F.M., Vaccaro M.S., Modelling issues and advances in nonlocal beams mechanics, *Int. J. Eng. Sci*.**,** 198: 104042, https://doi.org/10.1016/j.ijengsci.2024.104042.

54. Song Z.W., Lai S.K., Lim C.W., Li C., Theoretical examination for the consistency of Eringen's nonlocal theories in nanomaterial modeling, International Journal of Applied Mechanics, **17**(06): 2550044, 2025, https://doi.org/10.1142/S1758825125500449.
55. Pramanik D., Nobili A., A well-posed non-local theory in 1D linear elastodynamics, *International Journal of Solids and Structures*, **320**: 113511, 2025, https://doi.org/10.1016/j.ijsolstr.2025.113511.
56. Pisano A.A., Fuschi P., Polizzotto C., Euler–Bernoulli elastic beam models of Eringen's differential nonlocal type revisited within a continuous displacement framework, *Meccanica*, **56**: 2323-2337, 2021, https://doi.org/10.1007/s11012-021-01361-z.
57. Song Z.W., Lai S.K., Lim C.W,. A new insight into the paradoxical integral anddifferential constitutive relations of Eringen nonlocal theory, *J. Eng. Mech*., **151**: 04024112, 2025, https://doi.org/10.1061/JENMDT.EMENG-8021.
58. Song Z.W., Lai S.K., Lim C.W., On the truth of integral and differential constitutive forms in strain-driven nonlocal theories with bi-Helmholtz kernels for nanobeam analysis, *Thin-Walled Structures*, **214:** 113338, 2025, https://doi.org/10.1016/j.tws.2025.113338.
59. Song Z.W., Lai S.K., Lim C.W., On the nature of constitutive boundary and interface conditions in stress-driven nonlocal integral model for nanobeams, *Applied Mathematical Modelling*, **144**: 115949, 2025, https://doi.org/10.1016/j.apm.2025.115949.
60. Karličić D., Murmu T., Adhikari S., McCarthy M., [Ed.], *Nonlocal Structural Mechanics*, (Iste) (Kindle Location 636). Wiley. Kindle Edition, 2016.
61. Lu P., Lee H. P., Lu C., Zhang P.Q., Dynamic properties of flexural beams using a nonlocal elasticity model, Journal of Applied Physics, **99**: 073510, 2006, https://doi.org/10.1063/1.2189213.
62. Timesli A., Nonlocal buckling analysis of double-walled carbon nanotubes using Donnell shell theory, *Journal of Applied and Computational Mechanics*, **6**(3): 527-536, https://doi.org/10.22055/JACM.2020.32627.2004
63. Wang C.M. , Zhang Y.Y., Ramesh S.S., Kitipornchai S., Buckling analysis of micro- and nano-rods/tubes based on nonlocal Timoshenko beam theory, *Journal of Applied Physics*, **39**(17): 3904-3909, 2006, 10.1088/0022-3727/39/17/029.
64. Reddy J.N., Pang S.D., Nonlocal continuum theories of beams for the analysis of carbon nanotubes, *Journal of Applied Physics*, **103**: 023511, 2008, https://doi.org/10.1063/1.2833431.
65. Wang L., Hu H., Flexural wave propagation in single-walled carbon nanotubes, *Physical Review B - Condensed Matter and Materials Physics*, **71**(19): 195412, 2005, https://doi.org/10.1103/PhysRevB.71.195412.
66. Akpinar M., Uzun B., Yayli M.Ö., Dynamic response of axially loaded carbon nanotubes considering armchair, chiral, and zigzag configurations, *Mechanics Based Design of Structures and Machines*, 1-26, 2025, https://doi.org/10.1080/15397734.2025.2553325

67. Natsuki T., Endo M., Shi J. X., Nonlocal vibration characteristics of carbon nanotube resonators modeled as Euler-Bernoulli beams, *Nanomaterials*, **14**(2): 305, 2024, https://doi.org/10.3390/nano14020305.
68. Uzun B., Nonlocal vibration analysis of porous functionally graded nanobeams embedded in elastic medium, *Archive of Applied Mechanics*, **94**(3): 779-792, 2024. https://doi.org/10.1007/s00419-024-02559-3
69. Ebrahimi R., Chaotic vibrations of carbon nanotubes subjected to a traversing force considering nonlocal elasticity theory, *Proceedings of the Institution of Mechanical Engineers, Part N: Journal of Nanomaterials, Nanoengineering and Nanosystems*, **236**(1): 31–40, 2022, https://doi.org/10.1177/23977914211063309.
70. Murmu T., Pradhan S.C., Small-scale effect on the vibration of nonuniform nanocantilever based on nonlocal elasticity theory, *Physica E*, **41**: 1451-1456, 2009, https://doi.org/10.1016/j.physe.2009.04.015.
71. Wang C.M., Zhang Z., Challamel N., Duan W.H., Calibration of Eringen's small length scale coefficient for initially stressed vibrating nonlocal Euler beams based on microstructured beam model, *Journal of Applied Physics*, **46**: 345501, 2013, https://doi.10.1088/0022-3727/46/34/345501.
72. Khaniki H. B., Hosseini-Hashemi S., Buckling analysis of tapered nanobeams using nonlocal strain gradient theory and a generalized differential quadrature method, *Materials Research Express*, **4**(6): 065003, 2017, https://doi.10.1088/2053-1591/aa7111.
73. Thongyothee Ch., Chucheepsakul S., Postbuckling behaviors of nanorods including the effects of nonlocal elasticity theory and surface stress, *Journal of Applied Physics*, **114**: 243507, 2013, https://doi.org/10.1063/1.4829896.
74. Lu P., Lee H. P., Lu C., Zhang P.Q., Dynamic properties of flexural beams using a nonlocal elasticity model, *Journal of Applied Physics*, **99**: 073510, 2017, https://doi.10.1088/2053-1591/aa7111.
75. De Rosa M.A., Lippiello M., Luciano R., Vibration of nanocones modeled as nonlocal elastic beams with a concentrated mass, *Nanomaterials*, **11**(8): 2129, 2021, https://doi.org/10.3390/nano11082129.
76. Euler L., De motu columnarum erectarum, [in:] *Novi Commentarii academiae scientiarum Petropolitanae*, **10**: 99-140, 1757 (published 1759).
77. Bigoni D., *Nonlinear Solid Mechanics: Bifurcation Theory and Material Instability*, Cambridge University Press, 2012.
78. Manecka-Padaż A., Jenczyk P., Pęcherski R., Nykiel A., Experimental investigation of Euler's elastica: in-situ SEM nanowire post-buckling, *Bulletin of the Polish Academy of Sciences, Technical Sciences*, **70**(6): e143648, 2022, DOI: 10.24425/bpasts.2022.143648.
79. Dormand J.R., Prince P.J., A family of embedded Runge-Kutta formulae, *Journal of Computational and Applied Mathematics*, **6**(1): 19-26, 1980, https://doi.org/10.1016/0771-050X(80)90013-3.
80. Calvo M., Montijano J.I., Randez L., A fifth-order interpolant for the Dormand and Prince Runge-Kutta method, *Journal of Computational and Applied Mathematics*, **29**(1), 91–100, 1990.

81. Civalek Ö., Demir Ç., Bending analysis of microtubules using nonlocal Euler–Bernoulli beam theory, *Applied Mathematical Modelling*, **35**(5): 2053–2067, 2011, https://doi.org/10.1016/j.apm.2010.11.004.